THE NEW SPACE DEBRIS MITIGATION (SDM 4.0) LONG TERM EVOLUTION CODE

A. Rossi[1], **L. Anselmo**[1], **C. Pardini**[1], **R. Jehn**[2], **and G.B. Valsecchi**[3]

[1]*ISTI–CNR, Via Moruzzi 1, 54124, Pisa, Italy*
[2]*ESA-ESOC, Robert Bosch Str.5, 64293 Darmstadt, Germany*
[3]*INAF–IASF, Via del Fosso del Cavaliere 100, 00133 Roma, Italy*

ABSTRACT

The main new features in the Space Debris Mitigation long-term analysis program (SDM) recently upgraded to Version 4.0 are described. They include new or upgraded orbital propagators, two new collision probability algorithms, upgraded mitigation scenarios and new post-processing routines. The results of a set of simulations of the long term evolution of the Low Earth Orbit (LEO) environment are decribed. A No Future Launches, a Business as Usual and a Mitigated scenario are simulated, showing the need to adopt all the feasible proposed mitigation measures, in order to reduce the proliferation of orbiting debris. In particular, the mitigation measures proposed in this study appear capable of strongly reducing the growth of the 10 cm and larger population, but not enough to fully stabilize critical regions, such as the shell in the 800-1000 km altitude range.

1. INTRODUCTION

Originally developed in the early 90's under an ESA Contract [8] [1], the Space Debris Mitigation long-term analysis program (SDM) has been recently fully revised, redesigned and upgraded to Version 4.0. SDM 4.0 is now a full 3D LEO to GEO simulation code, including advanced features that make it perfect for long term studies of every orbital regime, with particular attention to the MEO and GEO regions. The structure and main assumptions of SDM were profoundly changed passing from Version 3.0 to Version 4.0, due to the increasing accuracy requirements in the modeling of the environment and thanks to the advancements in CPU power. The main characteristics of SDM, up to Version 3.0, can be found in [8] [1] [9]. A complete description of SDM 4.0 can be found in [10].

2. THE NEW FEATURES INSIDE SDM 4.0

The main change in the overall structure concerns the handling of the *historical population* and the collision probability evaluation. Up to SDM 3.0, the *historical population* was propagated only once (in a loop external to the main code) and was then handled only in terms of densities for the collision probability evaluation. The new, more sophisticated, collision probability evaluation algorithms are pair-wise processes working on actual target and projectile orbits, so the densities are no more suitable for this purpose. Therefore, in SDM 4.0, the objects in the *historical population* (i.e., the objects already present in space at the beginning of the run) are treated just like those in the *running population* (i.e., everything the is injected in space during the run) and their orbits are integrated within the run. The main physical quantity identifying an object in SDM 4.0 is the diameter (it used to be the mass up to SDM 3.0). This change was mainly dictated by the need to consistently adopt and implement the NASA breakup model [3], that is intrinsically based on object diameter. Area and mass are therefore now derived quantities.

The new or improved models added to the software are: i) a new orbital propagator (LEGO); ii) a revised versions of the Debris Cloud Propagator (DCP) and of the Fast Orbit Propagator (FOP); iii) two new algorithms for the collision probability evaluation (Öpik and CUBE); iv) new, advanced mitigation options and scenarios (including a new active removal algorithm); v) new post-processing routines, including a novel tool for the analysis of the collision risk for a spacecraft moved to a given disposal orbit.

2.1. Orbital Propagators

In SDM 4.0 three orbital propagators are implemented that can be selected according to the different orbital regimes and to the accuracy required. The Debris Cloud Propagator, is a very fast and efficient orbital propagator. Originally it included only the effect of the air drag. It allows an extremely fast propagation of a reduced set of orbital elements (semimajor axis, eccentricity and inclination) [1]. DCP was updated in SDM 4.0 so that it now propagates also the right ascension of ascending node Ω and the argument of perigee ω under the effect of the Earth oblateness, J_2.

Proc. '5th European Conference on Space Debris', Darmstadt, Germany
30 March – 2 April 2009, (ESA SP-672, July 2009)

The FOP orbital propagator was added to SDM 3.0. FOP (Fast Orbit Propagator) was originally developed as a stand alone code for the first SDM contract [1]. It is a very accurate propagator including all the relevant gravitational and non gravitational perturbations: geopotential harmonics, third body perturbations, solar radiation pressure (including shadows) and atmospheric drag. FOP uses the variation of parameters theory based on the integration of the Lagrange planetary equations of the orbital elements for geopotential, luni-solar perturbations and solar radiation pressure. In order to save CPU time, an analysis of the performances (in terms of accuracy vs. computing time) of FOP in different orbital regimes was performed. The aim was to optimize the choice of the parameters that control the accuracy of the orbital propagation, for every orbital regime. Therefore, in SDM 4.0 an ad-hoc set of control parameters is applied to every integrated orbit. Moreover, the possibility to run FOP integrating the whole set of 6 orbital elements (a, e, i, Ω, ω, M), or a reduced set of 5 elements, excluding the mean anomaly M, was introduced. In the last case the value of M is randomly drawn at the end of the FOP integration.

A third orbital propagator was added to SDM 4.0 to handle the orbits in, or close to, the geostationary regime. It is the LEGO (Long-term Evolution of Geostationary and near-geostationary Orbits) orbit propagator developed at ESOC. LEGO is based on averaging techniques by J.C. Van Der Ha [12]. It takes into account the perturbations due to the geopotential, the luni-solar gravitational attraction and the solar radiation pressure. Compared to the full integration of the motion equations taking into account the short-period terms, this orbit propagator gives a quite accurate orbit evolution within a very short computer-time.

2.2. Collision Probability Evaluation

SDM 4.0 uses two different approaches to calculate the collision rate between the orbiting objects. The user can select at the beginning of the run the desired algorithm.

The first method is based on Öpik's theory [11] and is a fully analytical algorithm that allows to evaluate the collision probability between objects in Low Earth Orbits (LEO). Öpik's theory makes basic assumptions that pose some caveats for its global application to the whole region of space considered by SDM 4.0. The Öpik approach is exact only if the target orbit is circular. It can be shown that it is still a good representation of the actual collision probability if the target eccentricity is below few percents. In SDM 4.0, due to the statistical nature of the process analyzed and to the approximations necessarily introduced in the simulation process, the Öpik approach can be applied to all targets whose eccentricity is below 0.1. Moreover, Öpik's theory assumes that the argument of perigee ω of the projectile orbit, evaluated using as reference plane the orbital plane of the target, is randomly distributed between 0 and 2π. This means, for instance, that the theory is not applicable to situations in which a resonance is constraining the distribution of ω, as is the case, for example, of the Molniya orbits. Nonetheless, in LEO, the randomization induced by the drift of ω due to the Earth's quadrupole J_2 is so effective that Öpik's theory can be safely applied without significant loss of accuracy. This does not apply to high Earth orbits (e.g., at the GPS altitude) where the precession rates $\dot{\omega}$ is about two orders of magnitude smaller than in LEO. This slower evolution prevents the direct application of our original method to Medium Earth Orbit (MEO). For this reason, in SDM 4.0 the Öpik approach can be applied only to orbits whose semimajor axis is less than $10\,000$ km.

The other collision probability evaluation algorithm implemented in SDM 4.0 is CUBE, developed at NASA/JSC [5]. It estimates the long-term collision probabilities by means of uniform sampling of the system in time and can be applied to any kind of orbit.

2.3. Mitigation Options

Since the first version of SDM a great effort was devoted into the design of a detailed traffic and mitigation model.

In SDM 4.0 the possibility to simulate new dedicated mitigation strategies was implemented to handle specifically the constellations of satellites and in particular the Navigation constellations in MEO. At end-of-life the satellites can be moved to a generic disposal orbit specified by a set of orbital elements (e.g., a graveyard orbit above the operational one). In the case of MEO constellations it was shown that the long term eccentricity growth of the disposed satellite can bring them back into the operational zone. Therefore, a disposal orbit whose argument of perigee ω minimizes the eccentricity growth can be targeted, by choosing ω in such a way that $\sin(2\omega + \Omega) \simeq +1$, that is $(2\omega + \Omega) \simeq 90^\circ$ [2].

The possibility to actively remove objects from space was already implemented in SDM 3.0. However, the algorithm implemented there was acting on the objects density, so it was no more suitable for SDM 4.0. The new algorithm allows the removal of specific objects based on a pre-defined criterion. Currently the criterion implemented is based on the size of the objects. A user-defined number (n_r) of the largest uncontrolled objects in LEO can be removed every year. The objects that can be removed must conform to the specifications described by the input parameters mentioned above and must be non-operational. Therefore, a preliminary check is done on all the objects in the run to identify all the non-operational objects. Then the non-operational objects are sorted by diameter and the n_r largest objects are removed (assuming a direct reentry in the atmosphere). It is worth stressing that the forced reentry of all the upper stages can be simulated by simply choosing appropriately the input variables of the launch routines.

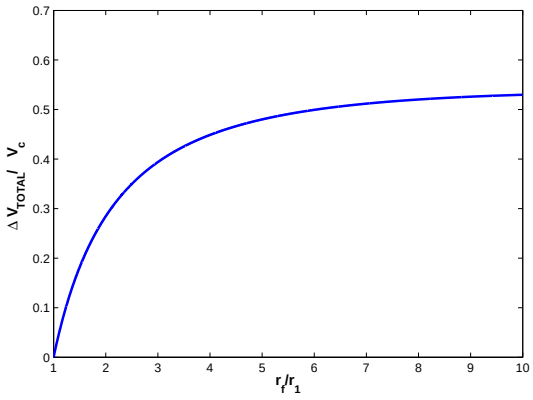

Figure 1. Relative ΔV required by a coplanar Hohmann transfer, as a function of the relative change in orbital radius.

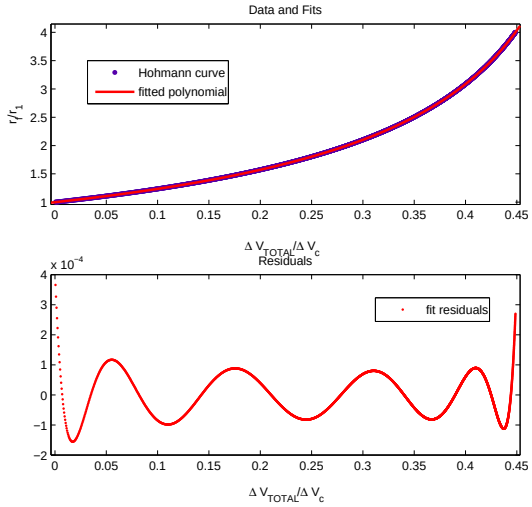

Figure 2. Polynomial fit to the function shown on Fig. 1. In the upper panel the blue dots are the values given by Fig. 1 and the red curve is the fitted polynomial. In the lower panel the residuals of the fit are shown.

2.4. Analysis of the Disposal Orbit Collision Risk

An analysis of the collision risk faced by a spacecraft once it is moved to a desired disposal orbit can be performed with SDM 4.0. This post-processing option works on the population files given in output by the different SDM 4.0 Monte Carlo runs and is designed to allow a preliminary understanding of the best disposal orbit in terms of residual collision risk for a given spacecraft.

In case of LEO or MEO, two disposal maneuvers are always simulated: a Hohmann transfer to a circular orbit with different altitude (performed with two impulsive burns) or a single burn disposal to an elliptic orbit with lower perigee. In Geostationary Earth Orbit (GEO) (or near GEO) the disposal maneuver is always a rising of the spacecraft to a circular orbit at the altitude dictated by the IADC Mitigation Guidelines.

The ΔV needed to change the altitude of an orbit with a two impulse Hohmann transfer (coplanar case) is given by:

$$\begin{aligned} \Delta V_{TOTAL} &= \Delta V_1 + \Delta V_2 = \\ &= V_c \left(\sqrt{\frac{2(r_f/r_1)}{1+(r_f/r_1)}} - 1 + \right. \\ &+ \left. \sqrt{\frac{1}{r_f/r_1}} - \sqrt{\frac{2}{r_f/r_1\,[1+(r_f/r_1)]}} \right) \end{aligned}$$

where:

V_C	circular velocity in the initial orbit;
r_f	radius of the final orbit;
r_1	radius of the initial orbit.

Fig. 1 shows the behaviour of $\Delta V_{TOTAL}/V_c$ as a function of r_f/r_i. The user has to provide a maximum ΔV and, from this input value, the maximum attainable r_f/r_i is calculated within the code. In order to do so, the plot in Fig. 1 is fitted with a 9^{th} degree polynomial:

$$\begin{aligned} r_f/r_1 &= p_1x^9 + p_2x^8 + p_3x^7 + p_4x^6 + p_5x^5 + \\ &\quad p_6x^4 + p_7x^3 + p_8x^2 + p_9x + p_{10} \end{aligned} \quad (1)$$

where $x = \Delta V_{TOTAL}/V_c$ and the coefficients p_n are the polynomial coefficients. Fig. 2 shows, in the upper panel, the fitting function (in red) and in the lower panel the residuals of the fit, giving a clear indication that the polynomial fit adopted is extremely accurate.

For a disposal to an elliptic orbit, with a single maneuver lowering the perigee, the required ΔV is given by:

$$\Delta V = \sqrt{GM_\oplus} \cdot \left(\sqrt{\frac{2}{r_a} - \frac{1}{a_i}} - \sqrt{\frac{2}{r_a} - \frac{1}{a_f}} \right) \quad (2)$$

where:

r_a	apogee radius of the initial orbit;
a_i	semimajor axis of the initial orbit;
a_f	semimajor axis of the final orbit;
$GM_\oplus$	gravitational constant times Earth mass.

and therefore the maximum change in eccentricity attainable with a given ΔV is:

$$\Delta e_{max} = \left(\frac{r_a}{a_f} - 1 \right) - e_i \quad (3)$$

where e_i is the eccentricity of the initial orbit.

Once the values of the attainable maximum changes, $\Delta h_{max} = r_i \pm |r_f - r_i|$ (the plus or minus signs refer to a raising or lowering maneuver, according to the orbital regime explored, e.g., GEO re-orbiting or LEO de-orbiting) and Δe_{max} are calculated, the software divides

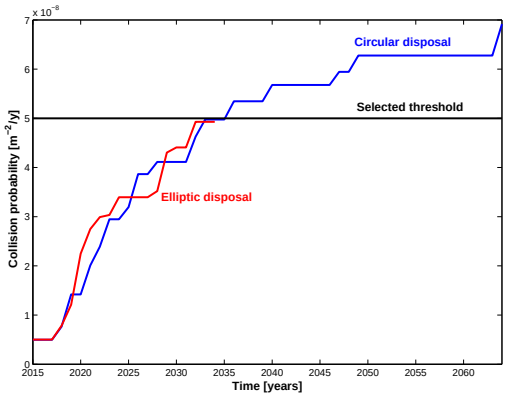

Figure 3. Sample plots of the disposal orbit collision risk analysis tool showing the time evolution of the cumulative collision probability for the two disposal orbits with the minimum final value in the cases of circular (blue curve) and elliptic disposal orbits (red curve). The horizontal line highlights the maximum allowed collision probability selected by the user, for ease of analysis.

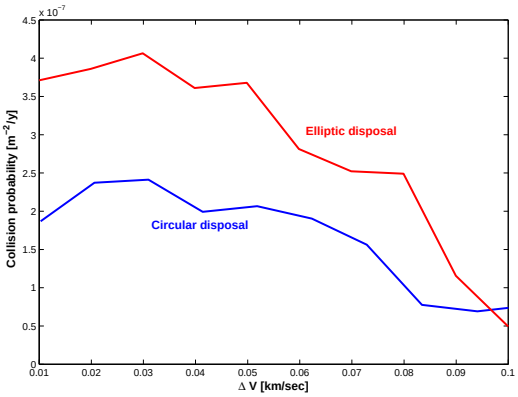

Figure 4. Sample plots of the disposal orbit collision risk analysis tool showing the value of the cumulative collision probability, as a function of the applied disposal maneuver ΔV in the case of elliptical disposal orbit (red curve) compared with the case of circular disposal orbit (blue curve).

the intervals in altitude and eccentricity in a given number of sub-intervals (10 as a default) Δh_n and Δe_n with $n = 1 \ldots 10$. For every value of Δh_n and Δe_n a disposal orbit is identified and is propagated for the desired time span (given in input) with FOP.

For every disposal orbit generated, the collision probability between the disposed spacecraft and the whole population of objects is calculated with the use of the CUBE algorithm. The timestep for the evaluation of the collision probability is set to 5 days.

At the end of the run, the disposal orbits (both in the case of elliptic and Hohmann transfer disposal) with the minimum collision probability, cumulated over the investigated time span, is plotted (see Fig. 3; note that the elliptic disposal orbit re-enters after 20 years and therefore the corresponding curve is truncated). Moreover, a number of plots showing the evolution of the collision probability is displayed. Fig. 4 shows the cumulative collision probability, as a function of the applied disposal maneuver ΔV_n with $n = 1 \ldots 10$ (corresponding to n values of Δe_n and Δh_n) for the case of elliptical disposal orbit, compared with the case of circular disposal orbit.

3. LONG TERM EVOLUTION STUDIES

The long term evolution of the space debris population in LEO was studied with the new SDM 4.0 package. The initial population adopted in all the scenarios described in this Section is MASTER 2005. Since the publication of the MASTER 2005 model, the major Feng Yun 1C collision profoundly modified the LEO environment. Therefore it was decided to add to the original population the fragments produced by this collision, as generated simulating the event with the same models adopted for the MASTER population. This population of fragments was kindly provided by H. Krag, (ESA/ESOC), and includes about $59\,000$ particles larger than 1 cm. The EVOLVE 4 explosion and collision models, and the CUBE collision probability algorithm were used. The orbits were propagated with FOP. The lower limit for the particles included in the simulations was 1 cm. The default explosion scenario includes an average number of 4.6 explosions per year. The number and the type of the events are taken from an analysis of the past 5 years. Each scenario was modeled with 20 independent Monte Carlo runs. In the following, the plots show the average from all the Monte Carlo runs, along with one standard deviation from the mean.

3.1. No Future Launches case

The No Future Launches (NFL) scenario is a typical study case to investigate the stability of the current debris environment. First devised in the early 90s' (see e.g. [7]) it came back to fashion recently after the publication of a few papers by Liou and Johnson [6].

The basic idea is to exclude the complex simulation of a credible future launch traffic (and explosion pattern) and let the system evolve, starting from the current population, having as the sole source of debris the mutual collisions between the objects already in orbit. The outcome of this simulation clearly gives an indication of the stability of the current environment with respect to the so-called *collisional cascade*, first predicted by Don Kessler [4].

The NFL scenario assumes that no mitigation measure is applied to the spacecraft already in orbit (i.e., no deorbiting is ever performed). Some residual explosions are allowed until the year 2015, at a rate of 4.6 events per

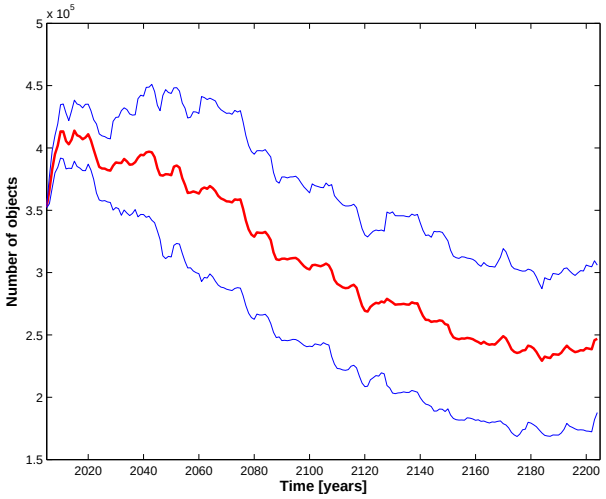

Figure 5. Number of LEO objects larger than 1 cm in the NFL case. The thin blue curves are the number of objects plus or minus 1σ.

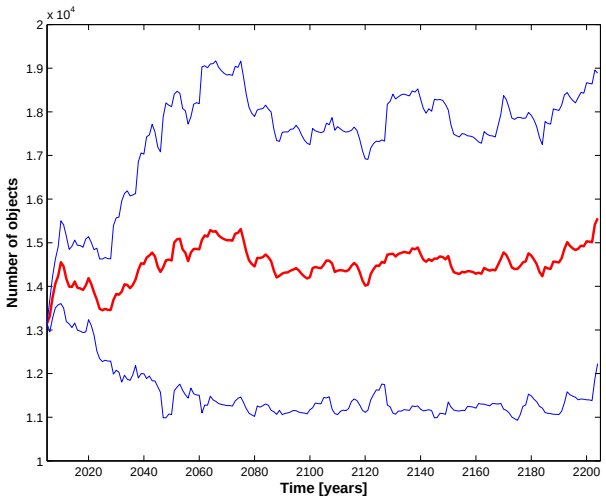

Figure 6. Number of LEO objects larger than 10 cm in the NFL case. The thin blue curves are the number of objects plus or minus 1σ.

year. In the year 2015 a complete stop to the explosions is applied. The simulation time span is 200 years.

Fig. 5 and Fig. 6 show the number of objects larger than 1 cm and 10 cm, respectively, as a function of time. After a short period of steady growth, due to the residual explosions, the population starts to decline, in both size regimes. The decline is much more pronounced in the 1 cm size regime, due mainly to the lack of slag particles that account for a considerable percentage of the MASTER 2005 initial population. On the other hand, for the 10 cm particles, after the initial decline, the population in LEO looks nearly stable, with a moderate increase toward the end of the simulation.

This is due to the increasing number of collisional debris as shown in Fig. 7. Fig. 8 shows the breakdown of the LEO population of objects larger than 10 cm, showing that the collisional debris become dominant in LEO after about 120 years.

Note that the collisional activity shown in Fig. 7 is well consistent with the one found by Liou and Johnson (see [6], Fig. 2). The majority of the collisions happens in the crowded altitude shell between 800 and 1000 km. It should also be noted how a significant number of collisions happens between large objects. Actually about 60% of the fragmentations involve intact spacecraft from the historical population. On the other hand, about 16% of the targets of all the fragmentations are fragments from previous collisions. It is also interesting to note that, on average, about 1 collision in every Monte Carlo run involves a fragment from the Feng Yun 1C event. In Fig. 9 the same breakdown of the population shown in Fig. 8 is plotted for the region between 900 and 1000 km, showing how in this region the collision debris become dominant already around the year 2060 and keep steadily increasing.

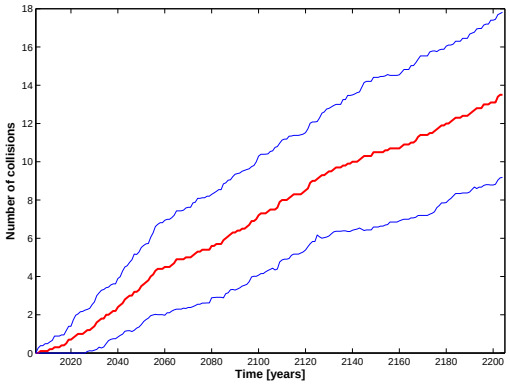

Figure 7. Cumulative number of collisions between LEO objects larger than 10 cm in the NFL case. The thin blue curves are the number of objects plus or minus 1σ.

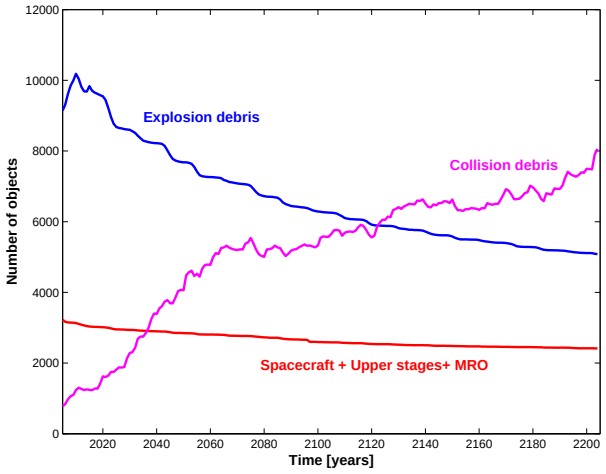

Figure 8. Breakdown of the number of LEO objects larger than 10 cm in the NFL case: intact objects (red line), explosion debris (blue line), collision debris (magenta line).

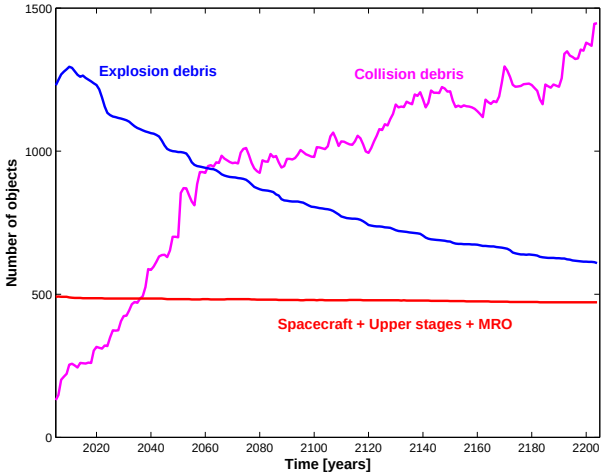

Figure 9. Breakdown of the number of objects larger than than 10 cm between 900 and 1000 km: intact objects (red line), explosion debris (blue line), collision debris (magenta line).

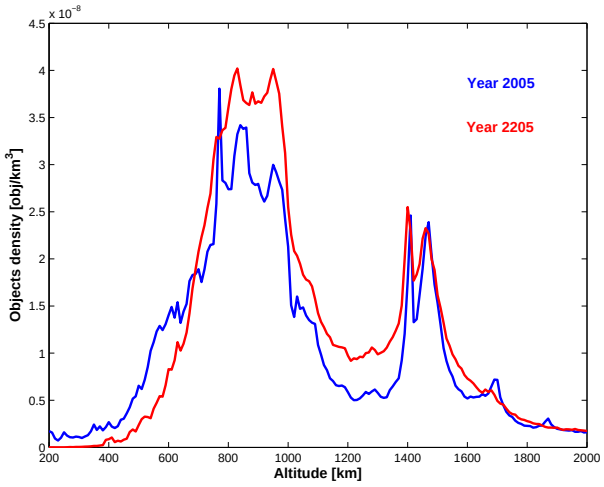

Figure 10. Density of objects larger than 10 cm in LEO at the beginning (blue line) and at the end (red line of the simulation time span.

Finally, Fig. 10 shows the density of objects larger than 10 cm in LEO at the beginning and at the end of the simulation time span. The significant increase of the population in the region between 800 and 1000 km can be noticed.

In summary, it can be concluded that the LEO population appears moderately unstable. I.e., even in the absence of new launches, in some regions of the LEO space the future collisions will continue to produce fragments that are increasing the overall number of objects and will sustain the collisional chain reaction. With respect to the results of [6], our simulations show a more moderate increase in the population. Nonetheless, it should be noticed that the MASTER 2005 population contains many more objects than those considered in [6], mainly in the size range very close to the 10 cm diameter. That is, while the overall collisional cross section in orbit is similar (leading to a comparable number of collisions over 200 years), our initial population is more difficult to "sustain" without launches, explosions and solid rocket motors slag injections. This partly accounts for the steeper pace observed in the Liou and Johnson plots.

3.2. Business As Usual and Mitigation Cases

In the last years the awareness of the space debris problem increased within the space operators. Some kind of mitigation measures became therefore widespread practices. These measures include, for example, the deorbiting or re-orbiting of spacecraft, the explosion prevention, the limited release of Mission Related Objects (MRO), etc.

For this reason, the Business As Usual (BAU) scenario simulated in this study, differently from other past studies, already includes some mitigation measures. It was deemed unrealistic to assume that for the next two centuries not even the mitigation measures already adopted could be applied.

The mitigation measures included even in the BAU case are: 1) re-orbiting of spacecraft in LEO at end-of-life, in an elliptic disposal orbit having a residual lifetime lower than 25 years (the so-called *25-year rule*), starting from the beginning of the simulation; 2) in-orbit explosion suppression starting from the year 2025. In the BAU case, all the upper stages (in every orbital regime) are instead left in orbit and occasionally a few mission related debris are released, according to current practices.

The launch traffic includes 45 *routine* launches, i.e. launches of spacecraft not related to a satellite constellation or to the International Space Station activities. The number and type of launches are taken from an analysis of the past 4.5 years of space activity. The maintenance of two of the currently existing LEO constellations, Iridium and Globalstar, is simulated. In the launch practices for these constellations, one launch per year is simulated, carrying 2 satellites in the case of Iridium and 4 satellites in the case of Globalstar. No constellation upper stage is

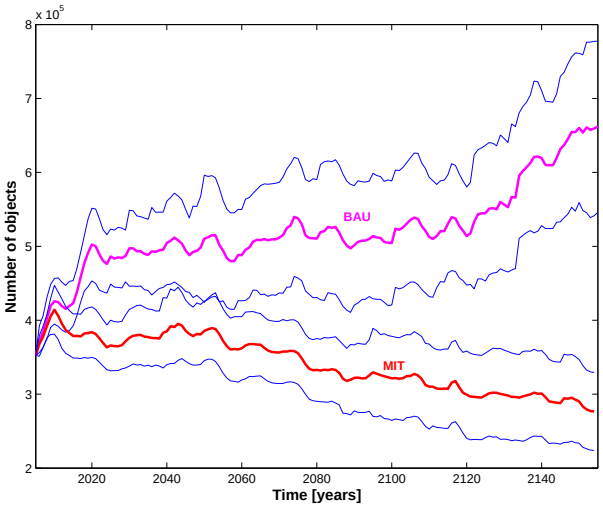

Figure 11. Number of LEO objects larger than 1 cm in the BAU (magenta line) and MIT (red line) cases. The thin blue curves are the number of objects plus or minus 1σ.

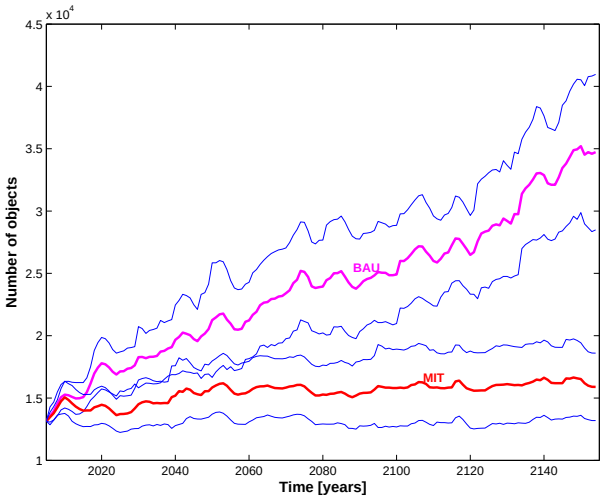

Figure 12. Number of objects LEO larger than 10 cm in the BAU (magenta line) and MIT (red line) cases. The thin blue curves are the number of objects plus or minus 1σ.

left in orbit. The lifetime of both the constellations is set to 20 years.

In the Mitigated (MIT) scenario the following differences with respect to the BAU case are introduced: the explosions are supposed to stop in the year 2010 and in all the routine launches no upper stage and no mission related debris is left in orbit after the year 2010. The simulation time span is 200 years, for both the analyzed scenarios.

Fig. 11 and 12 show the number of LEO objects larger than 1 cm and 10 cm, respectively.

From Fig. 12, it can be noticed how the adopted mitigation measures are able to strongly reduce the growth of the 10 cm population, with a mere 10% increase over 150 years. On the other hand, the BAU curve displays a more than linear growth that is a clear indication of the ongoing collisional activity.

Fig. 13 shows the cumulative number of collisions, resulting in catastrophic fragmentations, occurring in the two cases. Again the significant collisional activity related to the BAU case is apparent. The MIT case appears instead very close to the NFL case, showing how the comprehensive mitigation measures simulated are able to keep the debris population at a level similar to the present one. Fig. 14 shows how the altitude distribution of the fragmentations in the BAU and MIT cases is quite similar, despite the difference in absolute values, once more stressing the fact that the critical region is always the one between 800 and 1000 km, irrespectively of the simulation scenario adopted. It is worth stressing that whereas in the MIT case the region between 800 and 900 km and the region centered on 1000 km appears equally affected by collisional events, in the BAU case the vast majority of the events takes place in the lower region, due to many more feedback collisions.

Looking at the breakdown of the population of objects larger than 10 cm for the two cases under examination (BAU in Fig. 15 and MIT in Fig. 16), an overwhelming number of collisional debris in the BAU case can be noticed. In the BAU case the collision debris exceeds the explosion fragments already after about 50–60 years and in 130 years the population of collision fragments doubles the current explosion fragments population.

In conclusion, it can be stated that the operational practices must be revised, adopting all the feasible proposed mitigation measures, in order to reduce the proliferation of orbiting debris. In particular, the mitigation measures proposed in this study appear capable of strongly reducing the growth of the 10 cm and larger population, but not enough to fully stabilize critical regions, such as the shell in the 800-1000 km altitude range.

4. ACKNOWLEDGMENTS

The work described in this paper was carried out in the framework of the European Space Agency ESOC Contract No. 18423/04/D/HK to ISTI/CNR.

REFERENCES

[1] Anselmo, L., Cordelli, A., Farinella, P., Pardini, A. & Rossi, A. (1996). Final Report, Study on Long Term Evolution of Earth Orbiting Debris, ESA/ESOC Contract No. 10034/92/D/IM(SC), Consorzio Pisa Ricerche, Pisa, Italy.

[2] Jenkin, A.B. & Gick, R.A. (2003). Collision Risk Posed to the Global Positioning System by Disposal

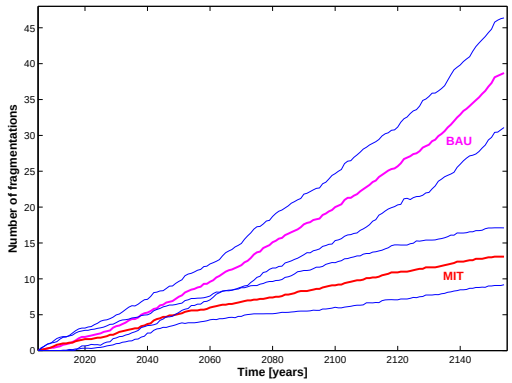

Figure 13. Cumulative number of collisions, resulting in catastrophic fragmentations, in the BAU (magenta line) and MIT (red line) cases. The thin blue curves are the plus or minus 1σ limits.

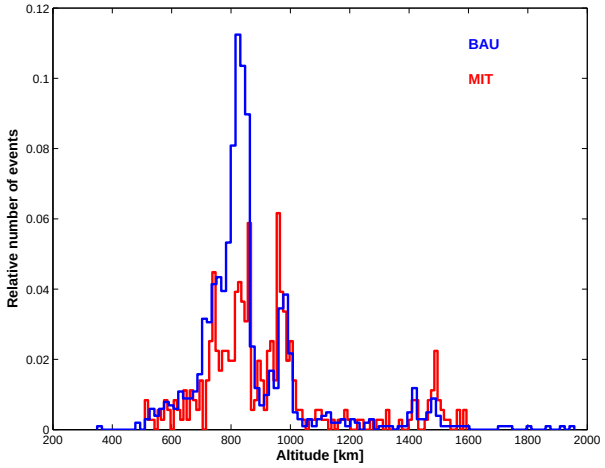

Figure 14. Distribution of the altitude of the collisional fragmentations, recorded in all the Monte Carlo runs, in the BAU (blue line) and MIT (red line) cases.

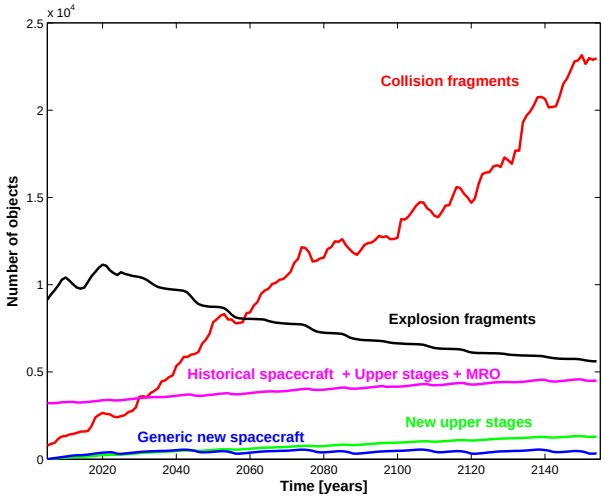

Figure 15. Breakdown of the population of objects larger than 10 cm in the BAU case.

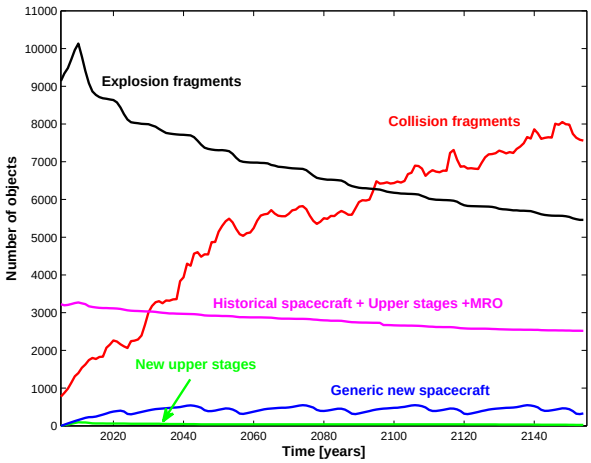

Figure 16. Breakdown of the population of objects larger than 10 cm in the MIT case.

Orbit Instability, *Journal of Spacecraft and Rockets*, **39** (4), 532–539.

[3] Johnson, N.L., Krisko, P.H., Liou, J.C. & Anz-Meador, P.D. (2001). NASA's New Breakup Model of EVOLVE 4.0, *Adv. Space Res.*, **28** (9), 1377-1384.

[4] Kessler, D.J. (1991). Collisional Cascading: the Limits of Population Growth in Low Earth Orbit, *Adv. Space Res.*, **11**, 63–66.

[5] Liou, J.-C. (2006). Collision Activities in the Future Orbital Debris Environment, *Adv. Space Res.*, **38**, 2102–2106.

[6] Liou, J.-C. & Johnson, N.L. (2008). Instability of the Present LEO Population, *Adv. Space Res.*, **41**, 1046–1053.

[7] Rossi, A., Cordelli, A., Farinella, P. & Anselmo, L. (1994). Collisional Evolution of the Earth's Orbital Debris Cloud, *Journal of Geophysical Research*, **99** (E11), 23195–23210.

[8] Rossi, A., Cordelli, A., Pardini, C., Anselmo, L. and Farinella, P. (1994). Modelling the Space Debris Environment: Two New Computer Codes, paper AAS 94-157, *Advances in the Astronautical Sciences*, Spaceflight Mechanics 1995, pp. 1217 – 1231, AAS Publication.

[9] Rossi, A., Anselmo, L., Pardini, C. & Valsecchi, G.B. (2004). Final Report, Upgrade of the Semi-Deterministic Model to Study the Long Term Evolution of the Space Debris. ESA/ESOC Contract No. 15857/01/D/HK(SC), ISTI/CNR. Pisa, Italy.

[10] Rossi, A., Anselmo, L., Pardini, C. & Valsecchi, G.B. (2009). Final Report, Semi-Deterministic Model. ESA/ESOC Contract No. 18423/04/D/HK, ISTI/CNR. Pisa, Italy.

[11] Valsecchi, G.B., Rossi, A. & Farinella, P. (2000) Visualizing impact probabilities of space debris, *Space Debris*, **1**, 143–158.

[12] Van Der Ha, J.C. (1986). Long Term Orbit Evolution of a Near-Geostationary Orbits, *J. Guidance Control and Dynamics*, **9**, 363–370.